

4

DTIC FILE COPY

MEMORANDUM REPORT BRL-MR-3791

BRL

AN ALGEBRAIC TURBULENCE MODEL
FOR FLOW SEPARATION CAUSED BY
FORWARD AND BACKWARD FACING STEPS

J. E. DANBERG
N. R. PATEL

DECEMBER 1989

DTIC
ELECTE
OCT 30 1989
S E D

APPROVED FOR PUBLIC RELEASE: DISTRIBUTION UNLIMITED.

U.S. ARMY LABORATORY COMMAND

BALLISTIC RESEARCH LABORATORY
ABERDEEN PROVING GROUND, MARYLAND

AD-A213 800

DESTRUCTION NOTICE

Destroy this report when it is no longer needed. DO NOT return it to the originator.

Additional copies of this report may be obtained from the National Technical Information Service, U.S. Department of Commerce, Springfield, VA 22161.

The findings of this report are not to be construed as an official Department of the Army position, unless so designated by other authorized documents.

The use of trade names or manufacturers' names in this report does not constitute indorsement of any commercial product.

REPORT DOCUMENTATION PAGE

Form Approved
OMB No. 0704-0188

1a. REPORT SECURITY CLASSIFICATION UNCLASSIFIED		1b. RESTRICTIVE MARKINGS	
2a. SECURITY CLASSIFICATION AUTHORITY		3. DISTRIBUTION / AVAILABILITY OF REPORT Approved for public release, distribution unlimited.	
2b. DECLASSIFICATION / DOWNGRADING SCHEDULE			
4. PERFORMING ORGANIZATION REPORT NUMBER(S) BRL-MR-3791		5. MONITORING ORGANIZATION REPORT NUMBER(S)	
6a. NAME OF PERFORMING ORGANIZATION U.S. Army Ballistic Research Laboratory	6b. OFFICE SYMBOL (if applicable) SLCBBR-LF	7a. NAME OF MONITORING ORGANIZATION	
6c. ADDRESS (City, State, and ZIP Code) Aberdeen Proving Ground, Maryland 21005-5066		7b. ADDRESS (City, State, and ZIP Code)	
8a. NAME OF FUNDING / SPONSORING ORGANIZATION	8b. OFFICE SYMBOL (if applicable)	9. PROCUREMENT INSTRUMENT IDENTIFICATION NUMBER	
8c. ADDRESS (City, State, and ZIP Code)		10. SOURCE OF FUNDING NUMBERS	
		PROGRAM ELEMENT NO. 61102A	PROJECT NO. 1L161102AH43
		TASK NO. 00	WORK UNIT ACCESSION NO. 001 AJ
11. TITLE (Include Security Classification) AN ALGEBRAIC TURBULENCE MODEL FOR FLOW SEPARATION CAUSED BY FORWARD AND BACKWARD FACING STEPS			
12. PERSONAL AUTHOR(S) DANBERG, JAMES E. and PATEL, NISHEETH R.			
13a. TYPE OF REPORT Memorandum Report	13b. TIME COVERED FROM _____ TO _____	14. DATE OF REPORT (Year, Month, Day)	15. PAGE COUNT
16. SUPPLEMENTARY NOTATION			
17. COSATI CODES			18. SUBJECT TERMS (Continue on reverse if necessary and identify by block number) Fluid Mechanics Separated Flow Supersonic Flow Turbulent Flow Turbulence Modeling Forward and Backward Steps Algebraic Model
FIELD	GROUP	SUB-GROUP	
01	20		
01	04		
19. ABSTRACT (Continue on reverse if necessary and identify by block number) The Baldwin-Lomax algebraic turbulence model is currently widely used in numerical Navier-Stokes codes primarily because it avoids the problems of calculating a boundary layer thickness. However, two of its disadvantages are: 1) it requires the evaluation of a maximum in the moment of vorticity with respect to the surface which is ambiguous under certain conditions and, 2) its applicability to some separated flows is unclear. The basis for the Baldwin-Lomax method is reviewed in detail particularly as it applies to locally separated flows. This leads to a reformulation of the Baldwin-Lomax method. The modification uses a velocity scale, at each separated flow station, which is the difference between the maximum velocity and the minimum velocity (considered negative in separated flows with recirculation regions). The length scale is defined in terms of the ratio of this velocity scale to the maximum vorticity. Other modifications are included which adapt the model to forward and rearward facing step applications. (CONTINUED ON REVERSE SIDE)			
20. DISTRIBUTION / AVAILABILITY OF ABSTRACT <input checked="" type="checkbox"/> UNCLASSIFIED/UNLIMITED <input type="checkbox"/> SAME AS RPT. <input type="checkbox"/> DTIC USERS		21. ABSTRACT SECURITY CLASSIFICATION UNCLASSIFIED	
22a. NAME OF RESPONSIBLE INDIVIDUAL James E. Danberg		22b. TELEPHONE (Include Area Code) (301) 278-4280	22c. OFFICE SYMBOL SLCBBR-LF-C

Table of Contents

	<u>Page</u>
List of Figures	v
I. INTRODUCTION	1
II. A BASIS FOR THE BALDWIN-LOMAX TURBULENCE MODEL	1
1. ATTACHED BOUNDARY LAYER	3
2. INCIPIENT SEPARATED FLOW	5
3. FULLY SEPARATED FLOWS	6
4. SUMMARY	7
III. MODIFICATION FOR STEP FLOWS	8
1. OUTER EDDY VISCOSITY	8
2. INNER LAYER EDDY VISCOSITY FOR FORWARD AND REAR- WARD FACING SURFACES	8
3. SEPARATION POINT	9
4. INTERMITTENCY	9
5. CONVEX CORNER	9
IV. ROTATING BAND APPLICATION	10
V. CONCLUDING REMARK	11
References	21
List of Symbols	23
DISTRIBUTION LIST	24



Accession For	
NTIS CRA&I	<input checked="" type="checkbox"/>
DTIC TAB	<input checked="" type="checkbox"/>
Unannounced	<input type="checkbox"/>
Justification	
By _____	
Distribution/	
Availability Codes	
Dist	Avail and/or Special
A-1	

INTENTIONALLY LEFT BLANK.

List of Figures

<u>Figure</u>		<u>Page</u>
1	Computational grid and model geometry (dimensions are in feet).	13
2	Comparison between computed and measured pressure distributions (Mach number = 3.0, $H/D = 0.04$, $Re = 1.33 \times 10^6$).	14
3	Mach number contours (dimensions are in ft).	15
4	Pressure contours in separated flow region ahead of band (dimensions are in feet).	16
5	Pressure contours in separated flow region behind band (dimensions are in feet).	17
6	Velocity vector plot (dimensions are in ft).	18
7	Velocity profile ahead of band ($\Delta X/H = 0.438$).	19
8	Velocity profile behind of band ($\Delta X/H = 0.10$).	20

INTENTIONALLY LEFT BLANK.

I. INTRODUCTION

There are many situations where there is a need to be able to compute turbulent flow over steps; both forward and backward facing. Some examples from the field of projectile aerodynamics include the flow over rotating bands, buttress threads and grooves on artillery shell. Another example is the internal flow around injector plates and flame-holders in ramjet propulsion systems. The use of Navier-Stokes computational techniques to compute the flow around protuberances, such as rotating bands on an artillery shell, has been attempted in which grid elements have been "blanked-out" to simulate the band.¹ The Baldwin-Lomax² turbulence model was employed in this application without modification. Although the results were encouraging there were a number of questions concerning the applicability of the turbulence model to local regions of separation caused by protuberances.

The following report attempts to consider some of these conceptual difficulties associated with the Baldwin-Lomax method. The first section investigates the basis for the method with the aim of understanding its limitations. In the subsequent sections, an algebraic turbulence model is proposed for protuberance induced separated flows which is an extension of the Baldwin-Lomax model. The new model is incorporated into an explicit, axisymmetric Navier-Stokes solver developed by Patel.³ This solver uses the MacCormack predictor-corrector method in a zonal scheme which is particularly well suited to computation of flows over geometries with sharp corners. The technique is then applied to a cone-cylinder-protuberance configuration for which wind tunnel pressure distribution measurements are available.

II. A BASIS FOR THE BALDWIN-LOMAX TURBULENCE MODEL

The underlying assumptions are that the turbulent eddy viscosity, μ_t , is a scalar variable dependent only on local conditions (i.e., diffusion and convection of turbulence are not specifically taken into account). Given the eddy viscosity, the effective turbulent stresses in the mean flow equations can be computed for local values of the strain rate. All these assumptions are common to most isotropic algebraic turbulence models. In addition, the Baldwin-Lomax method is a two layer model composed of a wall layer based on Prandtl's mixing length with Van Driest damping near the wall and an outer layer based on a nearly constant eddy viscosity in the fully turbulent 'wake' region.

The wall layer, as formulated in reference (2), is described by the following formula:

$$\mu_t^i = \rho \ell^2 |\omega|. \quad (1)$$

where:

μ_t^i = inner layer eddy viscosity ,

ρ = density ,

ℓ = $\kappa y [1 - \exp(-y^+/A^+)]$,

where the square bracket term is Van Driest's damping factor

$|\omega|$ = magnitude of the vorticity ,

y^+ = $u_\tau y / \nu_w$,

A^+ = 26.0 (Nondimensional damping parameter = $u_\tau A / \nu$),

u_τ = shear velocity, $\sqrt{\tau_w / \rho_w}$

y = distance normal to the wall ,

κ = 0.4 (von Karman constant) .

This is the same as the earlier Prandtl-Van Driest mixing length approach except that the derivative of the velocity with respect to the normal to the wall is replaced by the vorticity.

In the outer region of a viscous layer two formulations are proposed, one for attached boundary layers and the other for wake-like separated flows. The turbulent viscosity is taken to be the smaller of the following two values:

(1.)

$$\mu_t^o = K C_{cp} \rho y_m F(y_m) \gamma, \quad (2)$$

where:

$F(y)$ = $y |\omega| [1 - \exp(-y^+/A^+)]$,

$F(y_m)$ = maximum of $F(y)$ where y_m is the normal distance to the point where $F(y)$ is maximum ,

K = 0.0168 ,

C_{cp} = 1.6 ,

γ = $[1 + 5.5(C_{kleb} y/y_m)^6]^{-1}$ (Klebanoff intermittency factor),

C_{kleb} = 0.3 (note: original form for γ implies⁴ $C_{kleb} = y_m/\delta$).

(2.)

$$\mu_t^* = K \rho C_{cp} C_{uk} [U_d^2 y_m / F(y_m)]^\gamma, \quad (3)$$

where:

$$U_d = \sqrt{(u^2 + v^2 + w^2)_{max}} - \sqrt{(u^2 + v^2 + w^2)_{min}},$$

$$C_{uk} = 0.25.$$

Note that the second term in the U_d equation is zero for all wall flows if the no slip boundary condition is applied at the wall. This is because the velocity components are squared. Such a form is more appropriate for wakes or jet flows where the U_d is the difference between two positive velocities. For separated wall flows which involve some upstream flow, the minimum velocity is usually considered negative relative to the maximum velocity. If the velocity scale is interpreted as the difference between the maximum and minimum velocity, then U_d is larger than the maximum velocity.

Since these equations are intuitive, phenomenological hypotheses, they can not be derived with rigor. The original Baldwin and Lomax² paper did not include any derivations. However, some aspects can be related to well known empirical descriptions of turbulent shear flows. In the following sections the relationship to turbulent velocity profile characteristics is developed and discussed with the objective of defining the applicability of the method to separated flows over step geometries.

A significant part of the following development has to do with the evaluation of the parameters C_{cp} , C_{uk} (or more correctly the product $C_{cp}C_{uk}$) and C_{kleb} . These parameters are shown to be related to the parameters of the boundary layer profiles considered. However, it should be kept in mind that Baldwin and Lomax determined the values for these parameters by comparing numerical results with data from a transonic shock-separated flow experiment. Thus, the parameters are probably not universal, but depend on the Mach number range, pressure gradient and possibly other conditions which have yet to be identified.

1. ATTACHED BOUNDARY LAYER

A starting point is to consider incompressible, two-dimensional boundary layers. In that case, Clauser⁵ has established that the outer layer eddy viscosity can be described by the formula:

$$\mu_t^* = K \rho U_e \delta_k^*, \quad (4)$$

where

$$\delta_k^* = \int_0^\delta (1 - u/U_e) dy,$$
$$K = 0.0168.$$

This formula is usually used to determine the maximum of the eddy viscosity. Equation (4) is then multiplied by the Klebanoff intermittency factor to account for the decrease in

μ_i^0 as the inviscid external flow is approached.

Coles^{6,7} has proposed the following single empirical equation for the velocity profile which unifies the wall and wake regions except for the region immediately adjacent to the wall (the laminar sublayer).

$$u = u_\tau \left[\frac{1}{\kappa} \ln(y^+) + B + 2 \frac{\Pi}{\kappa} \sin^2 \left(0.5\pi \frac{y}{\delta} \right) \right], \quad (5)$$

where:

B = wall layer constant, normally 5.0 to 5.5,

Π = wake layer parameter (function of pressure gradient),

δ = boundary layer thickness.

The main difficulty with this equation is in the proper evaluation of δ which is somewhat arbitrary because of the asymptotic disappearance of viscous effects at large distances from the wall. The Baldwin-Lomax method is an attempt to circumvent the necessity for the direct evaluation of the boundary layer thickness.

In a wall bounded viscous flow, sufficiently far from the separation point so that over most of the boundary layer the Van Driest damping factor is unity, the vorticity is primarily du/dy . Thus, the function $F(y)$ can be formed as follows:

$$F(y) = y \frac{du}{dy} = u_\tau \left[\frac{1}{\kappa} + \left(\frac{4\Pi}{\kappa} \right) (\sin \eta \cos \eta) \eta \right], \quad (6)$$

where $\eta = 0.5\pi y/\delta$. This quantity has the dimensions of velocity and primarily describes the moment of wake vorticity with respect to the surface. The maximum in $F(y)$ is defined by a unique value of η denoted by η^* . The value of η^* can be determined from the following implicit equation which is obtained by setting $dF/d\eta = 0$.

$$\sin \eta^* \cos \eta^* + (1 - 2 \sin^2 \eta^*) \eta^* = 0.$$

Thus η^* is found to be:

$$\eta^* = 1.014375.$$

Since $y = y_m$ at that point, δ is seen to be directly proportional to y_m .

$$\delta = 1.548 y_m. \quad (7)$$

This result determines the constant in the intermittency function for attached flows as:

$$C_{kleb} = \frac{y_m}{\delta} = 0.6460. \quad (8)$$

Coles profile law, equation (5), can be integrated to provide a relationship between δ_k^* and δ as:

$$\delta_k^* = \delta \frac{(1 + \Pi)}{\left[\kappa \left(\frac{U_\tau}{u_\tau} \right) \right]}. \quad (9)$$

Thus

$$U_\epsilon \delta_k^* = \frac{1 + \Pi}{\kappa} u_\tau \frac{\pi y_m}{2 \eta^*} \quad (10)$$

Finally u_τ can be eliminated in favor of $F(y_m)$ by using equation (6) so that Clauser's wake eddy viscosity becomes identical with equation (2) if:

$$C_{cp} = \frac{(1 + \Pi) \pi}{2[1 + 4\Pi(\sin \eta^* \cos \eta^*) \eta^*]} \quad (11)$$

The pressure gradient parameter, Π , cannot be specified in a general way. Coles estimated Π to be 0.55 for flat plates at high Reynolds number. For equilibrium turbulent boundary layers, White⁸ has correlated Π in terms of the external flow pressure gradient from a number of experiments in the following form:

$$\Pi = 0.8(\beta + 0.5)^{0.75}, \quad (12)$$

where

$$\beta = \left(\frac{\delta^*}{\tau_w} \right) \frac{dp_\epsilon}{dx}$$

and dp_ϵ/dx = the pressure gradient at the edge of the boundary layer. For accelerating flows, the pressure gradient and β are negative with the limiting condition being $\Pi=0$. On the other hand, for decelerating flows with positive pressure gradients, there is no limit to the magnitude of β or Π because τ_w , the wall shear stress, approaches zero as the flow approaches separation. Thus, the limiting conditions of Π for attached flows can be identified and the corresponding values of C_{cp} calculated from equation (11).

$$\left. \begin{array}{l} \Pi = 0, \quad C_{cp} = \frac{\pi}{2} = 1.549 \\ \Pi = 0.55, \quad C_{cp} = 1.2 \\ \Pi = \infty, \quad C_{cp} = \frac{\pi}{8 \sin \eta^* \cos \eta^* (\eta^*)^2} = 0.8510 \end{array} \right\} \quad (13)$$

This is to be compared to the value of C_{cp} of 1.6 recommended by Baldwin and Lomax.

An analysis similar to the above has been reported by Granville.⁹ He employed a different form for the Coles wake function which was developed by Moses.¹⁰ In addition, a correlation by Nash¹¹ was used to connect the wake parameter Π to the pressure gradient. The consequence of Granville's analysis is to show that C_{cp} varies with Π in basically the same manner as obtained here in equation (11). However, the form of the wake function Granville used results in C_{kleb} (i.e. y_m/δ) also being a function of Π which is not the case, when the original Coles' wake function is used.

2. INCIPIENT SEPARATED FLOW

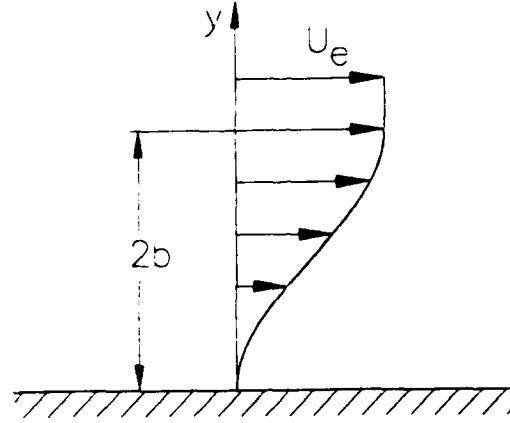
It is assumed that the velocity profile for incipient separated flow can be described by the limiting form of equation (5) as Π becomes large and the wall shear stress, τ_w (i.e., u_τ) goes to zero. The logarithmic and constant wall function terms go to zero but the coefficient of the sine term has the following limiting value:

$$\lim_{\tau_w \rightarrow 0} \frac{2u_\tau \Pi}{\kappa} = U_\epsilon \quad (14)$$

Thus, the incipient profile can be written as:

$$u = U_e \sin^2 \left(\frac{\pi y}{4b} \right),$$

where δ has been redefined in terms of b , the half width of the shear layer. In this case the



displacement thickness equals the half width, b . The function $F(y)$ becomes:

$$F(y) = y \frac{du}{dy} = 2U_e (\sin \eta \cos \eta) \eta.$$

$F(y_m)$ corresponds again to $\eta = \eta^* = 1.014375$ and

$$b = \pi \frac{y_m}{4\eta^*}. \quad (15)$$

The Clauser wake eddy viscosity becomes the same as equation (2):

$$\mu_t^o = K C_{cp} \rho y_m F(y_m) \gamma,$$

where $C_{cp} = 0.8510$ which is identical to the $\Pi \rightarrow \infty$ limit for the attached boundary layer case, as computed earlier in equation (13).

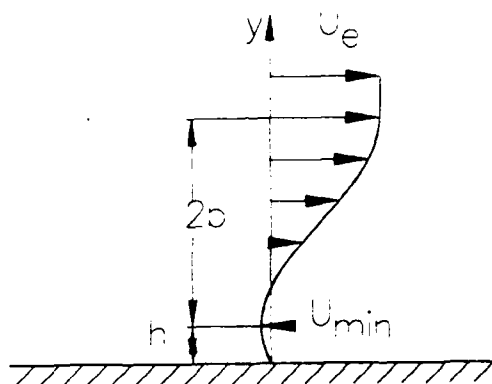
3. FULLY SEPARATED FLOWS

Next consider a fully separated region in which the shear layer is displaced a distance h away from the wall as shown in the following sketch. The shear layer of width $2b$ is now taken to extend from the minimum to the maximum velocity. The location of the maximum in $F(y)$, relative to the surface, is no longer proportional to b , the half width of the shear layer.

The shear layer velocity distribution is assumed of the same form as the incipient profile but translated a distance h from the wall. Thus, the sine squared profile starts at the minimum velocity location rather than the wall. The shear layer profile is approximated by:

$$u = U_{min} + U_d \sin^2 \left[\frac{\pi(y-h)}{4b} \right];$$

for $y \geq h$, where $U_d = U_{max} - U_{min}$ ($U_{min} < 0$).



The maximum velocity gradient, $\partial u / \partial y$, occurs at $y = h + b$ so that,

$$b = \pi \frac{U_d}{\left[4 \left(\frac{\partial u}{\partial y} \right)_{max} \right]} \quad (16)$$

This relation can be put into a form consistent with that of Baldwin and Lomax by taking $y_m \approx h + b$ and $F(y_m) \approx (h + b)(\partial u / \partial y)_{max}$. Therefore, the length scale for the outer flow can be written as:

$$b \approx \frac{\pi U_d}{4} \frac{y_m}{F(y_m)} \quad (17)$$

Thus the turbulent viscosity becomes (see Equation (3)):

$$\mu_t^o = K \rho C_{cp} C_{uk} \left[\frac{U_d^2 y_m}{F(y_m)} \right] \gamma.$$

where $C_{cp} C_{uk} = 0.25\pi$ and if $C_{cp} = 0.8510$, then $C_{uk} = 0.9229$. This should be compared to the value recommended by Baldwin and Lomax of 0.25. Although a value of $C_{uk} = 1.0$ is currently in use in some versions of the implicit Parabolized Navier-Stokes code.

4. SUMMARY

In the above sections, the outer layer eddy viscosity formulas of Baldwin and Lomax have been related to the velocity profile characteristics through the use of Coles law of the wall and wake. This was done in order to show how the Baldwin-Lomax formulas can be derived from existing semi-empirical information and to clarify the approximations and limitations of their equations. For separated flow, a significant approximation is made in going from equation (16) to equation (17). Thus, in the following application, the outer layer characteristic length will be computed based on equation (16). This is consistent with the spirit of the Baldwin-Lomax method but avoids some of the limitations.

III. MODIFICATION FOR STEP FLOWS

In applying the above theory to the flow over forward and backward facing steps several new problems arise. Some of these are that: 1) the $F(y)$ function can have several maxima and minima and it is difficult to numerically program to find the correct maximum, 2) wall damping effects must be provided from more than one nearby wall, 3) the implementation of the intermittency factor should account for the displacement of the shear layer away from the wall by the recirculation zone and, 4) the Van Driest wall damping factor should not go to zero at the separation point.

The Navier-Stokes code, in which the new turbulence model is implemented, uses a grid which divides the flow region along the body into several zones. In two dimensional or axisymmetric flows, the grid can be designed so that the step geometry is defined in terms of constant grid lines. The x coordinate runs parallel to the main flow direction and y normal to it. The code marches in time and thus the calculation of the turbulent viscosity lags one time step behind the solution of the mean flow equations.

On walls with attached flow the conventional Baldwin-Lomax method is used. When any reversed flow (i.e., negative velocity relative to the freestream) is detected at any given station, the separated flow computation is invoked. Reversed flow exists when the velocity component parallel to the local surface, at any point on a normal from the wall, is negative relative to the main flow direction.

1. OUTER EDDY VISCOSITY

The difficulty with multiple maxima is eliminated by returning to the basis for the separated flow length scale. Instead of defining it in terms of the ratio of $y_m U_d / F(y_m)$ (see Equation (3)), one half of the ratio of the maximum velocity difference to the absolute value of the maximum vorticity is used. The search for the maximum vorticity starts at the minimum in the velocity. This assumes that the vorticity associated with the free shear layer is the largest and the shear layer determines the outer length scale. Thus the outer length scale is calculated from:

$$b = 0.5 \frac{U_d}{|\omega|_{max}}, \quad (18)$$

and the outer eddy viscosity is given by:

$$\mu_i^o = K C_{cp} U_d b \gamma. \quad (19)$$

2. INNER LAYER EDDY VISCOSITY FOR FORWARD AND REARWARD FACING SURFACES

Near any lateral wall, the Prandtl-Van Driest inner layer eddy viscosity takes over whenever it is less than the outer layer viscosity. The surfaces normal to the main flow direction also introduce a wall layer effect and the corresponding eddy viscosity associated

with such surfaces is calculated as.

$$\mu_{xt}^i = \rho (\kappa x_n)^2 |\omega| \left[1 - \exp \left(\frac{-x_n^+}{A^+} \right) \right]^2, \quad (20)$$

where x_n is the normal distance for these surfaces. The eddy viscosity, then, is the smaller of three quantities: μ_i^o , μ_{yt}^i or μ_{xt}^i .

3. SEPARATION POINT

Computation of the inner layer eddy viscosity and determination of $F(y_m)$ involves an additional problem when passing from the attached to separated flow because the wall shear stress goes to zero at that point. The Van Driest damping parameter, A , also goes to zero and the overall viscosity reduces to an unrealistically low value associated with laminar flow. This problem was observed by Visbal and Knight.¹² In the present case, the computed wall damping layer height, A , is restricted as follows:

$$A = \left[\left(\frac{u_\tau}{26\nu_u} \right) + \frac{G}{\delta} \right]^{-1}. \quad (21)$$

The added term, G/δ , remains finite when u_τ goes to zero. Thus, the maximum value of A is limited to $1/G$ of the total thickness of the shear layer, δ . A tentative value of three has been selected for G . The value of δ is taken as the normal distance from the wall to where u_ϵ occurs.

4. INTERMITTENCY

A problem arises in applying the intermittency factor because the shear layer can be displaced some distance away from the wall. If γ is calculated as a function of y/δ , the intermittency is too high at the outer edge of the shear layer. This can be corrected by making $\gamma = 1.0$ for all values of y less than the $y_m - b$, where y_m is now the location of the maximum vorticity. At larger values of y we use:

$$\gamma = \left\{ 1.0 + 5.5 \left[\frac{(y - y_m + b)}{2b} \right]^6 \right\}^{-1}, \quad y > (y_m - b). \quad (22)$$

Thus the intermittency factor starts to reduce the eddy viscosity at the inner boundary of the shear layer and falls to approximately the same level at the shear layer outer edge as it would at the outer edge of an attached boundary layer.

5. CONVEX CORNER

Another difficulty occurs near the top of a forward or backward step because it is not clear how to evaluate the inner layer eddy viscosity in that region. As previously described, the inner layer vorticity and Van Driest damping are computed along a normal to the local

wall. However, these properties in the flow opposite a convex corner (such as above and ahead of the corner of a forward facing step) can not be reached by a normal to either wall. In order to prevent there being a large discontinuous change in the eddy viscosity in this region, the normal distance (x_n in Equation (20)) is taken as the radial distance from the corner. The shear velocity is allowed to change linearly with the angle from one surface to the adjacent one.

IV. ROTATING BAND APPLICATION

Experiments have been performed which measure the pressure caused by supersonic flow over a rectangular band on a cone-cylinder wind tunnel model.¹³ A comparison has been made between the predicted pressure distribution and these observations. Other characteristics of the flow such as velocity profiles and contour plots of the mean flow variables are used to illustrate the quality of the results of the analysis.

Figure 1 shows the grid used for the computations and it also indicates the experimental geometry. The wind tunnel model consists of a 13.1° half angle cone followed by a seven caliber cylinder (1 caliber=25.4 mm). The Mach number was 3.0 and the wind tunnel Reynolds number was 1.3×10^6 , based on body diameter. In the experiments a rectangular cross section band, of thickness $H=1$ mm and width of 1.27 mm, was movable relative to fixed pressure taps. This allowed the pressure disturbance caused by the band to be measured with considerable detail in the nearly constant pressure region on the cylinder.

The computed pressure distribution is compared with the measurements in Figure 2. The agreement is very good ahead of the band, near the forward facing step, but underpredicts the pressure level behind the band. The minimum pressure is in fairly good agreement with the data but after the initial rise, the recovery toward the nearly ambient value is computed to be slightly less than that observed in the experiment.

Figure 3 shows the Mach number contours obtained by combining the results from the three separate grids.

Pressure contours ahead of and behind the band are shown in Figures 4 and 5. These show the compression and expansion waves generated by the flow moving over the separated zones. As expected the pressure on the forward face of the band reaches a maximum value of three times ambient near the top of the band where the shear layer flow reattaches. The mean pressure on the front face of the band is approximately 15% greater than the pressure on the cylinder just in front of the band. The pressure on the back face of the step is nearly constant; close to the minimum pressure. Except near the leading edge, the pressures on top of the band are very close to the ambient value.

The velocity vector plot of the flow in the three zones is shown in Figure 6. This plot clearly shows the recirculation regions near the band. Finally velocity profiles at two stations are shown in Figures 7 and 8. Figure 7 shows the profile at a point 0.438 step heights ahead of the band. The velocity is seen to fall very rapidly near $y = 0$ to its minimum value of -250 ft/s and then increase more slowly. The second of these figures

shows results close behind ($x/H = 0.10$) the band. Note the complicated variation of velocity close to the cylinder wall followed by a very thin shear layer coming off the top of the band. The viscous boundary layer is above the thin shear layer. Since the turbulent viscosity in the inner layer is essentially proportional to du/dy , it exhibits several local maxima at the inflection points and zero's at the minimums and maximums. Thus it is not surprising that the search for the correct maximum in the Baldwin-Lomax function, $F(y)$, is difficult to incorporate into a numerical code.

V. CONCLUDING REMARKS

The Baldwin-Lomax algebraic eddy viscosity model has been reviewed and a basis for the separated flow formulation has been developed using an assumed form for the separated flow velocity profile. This analysis of the Baldwin-Lomax model has been undertaken in order to clarify its applicability and its limitations with regard to the use in Navier-Stokes computations of step induced separation. One conclusion which can be drawn is that the length scale is associated with the ratio of velocity scale to the maximum velocity gradient (or vorticity). Numerical computations can be based on this formulation rather than using the Baldwin-Lomax variables, $F(y_m)$ and y_m .

Several other modifications of the Baldwin-Lomax method have been suggested and implemented for the flow over forward and backward facing steps. These include: 1) providing for damping effects on the forward and backward faces of the step, 2) accounting for the displacement of the shear layer in implementation of the intermittency factor, 3) modification of the Van Driest damping function so that it does not become unrealistic at the beginning of separation or reattachment.

The modified turbulence model was incorporated into an explicit Navier-Stokes code which is designed to compute the flow in zones. This feature makes the code particularly suitable for application to the flow over steps. The test case which has been computed using this code is that of a cone-cylinder model with a simulated rotating band. The rotating band provides a rectangular forward and rearward facing step to the local flow. The configuration has been tested in a wind tunnel and detailed pressure distributions are available for comparison with the computed results.

The results of the comparison show that the pressure distribution ahead of the band is well predicted. The extent of the computed separated zone agrees with experiment as well as the form and magnitude of the pressure distribution. Behind the band the results are less satisfactory in that the pressure recovery from the minimum is too rapid. The minimum pressure and the extent of the recovery region are correct but the pressure at reattachment and downstream are slightly lower than experimentally observed. This result agrees with other Navier-Stokes computations using the un-modified Baldwin-Lomax method with a grid blanking technique to model the rotating band.

Additional testing of the turbulence model on other flow situations will be required in order to tune the empirical constants and investigate the range of the models applicability. The results shown here indicate that simple algebraic models can be used in at least some

complex flows.

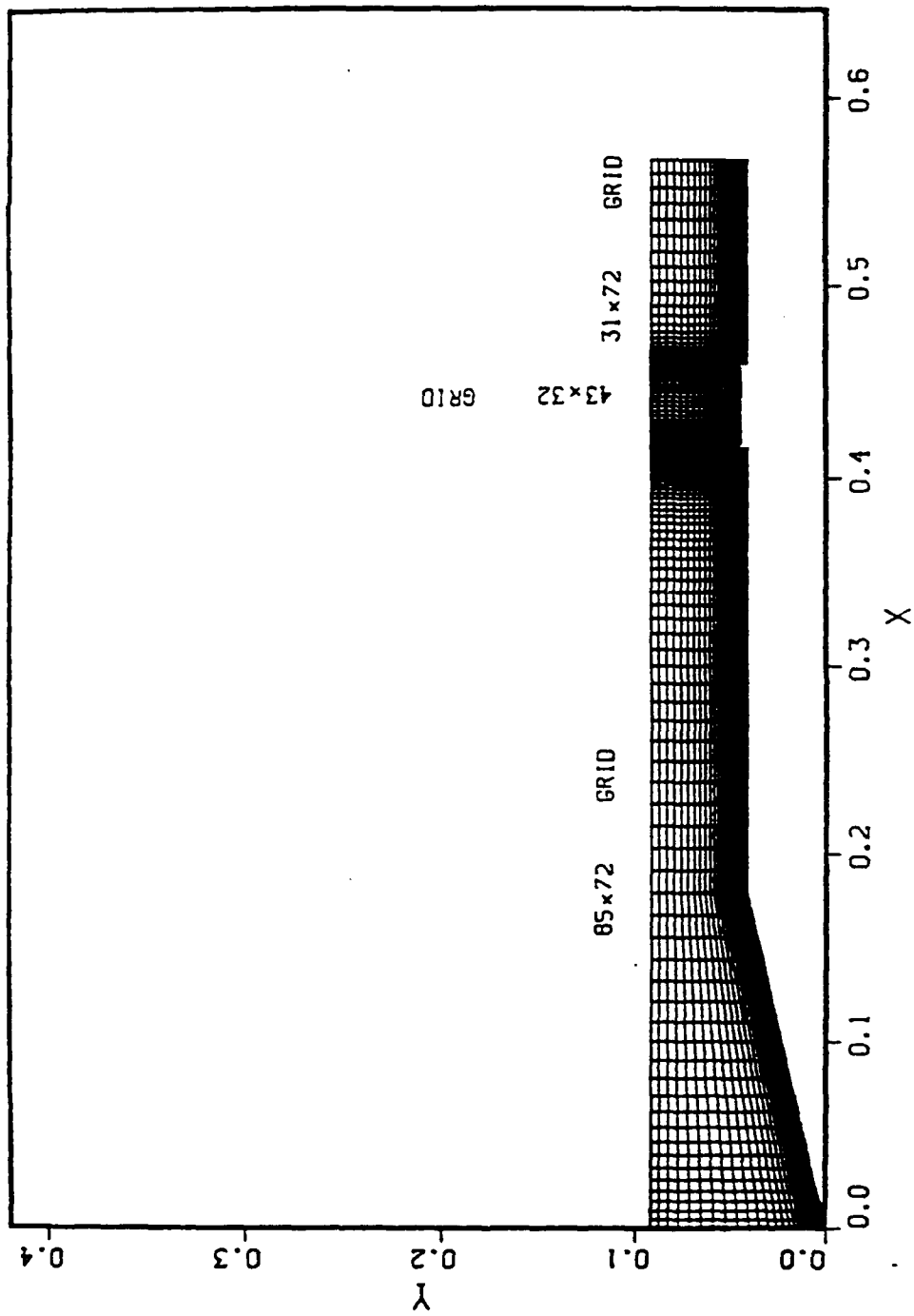


Figure 1. Computational grid and model geometry (dimensions are in feet).

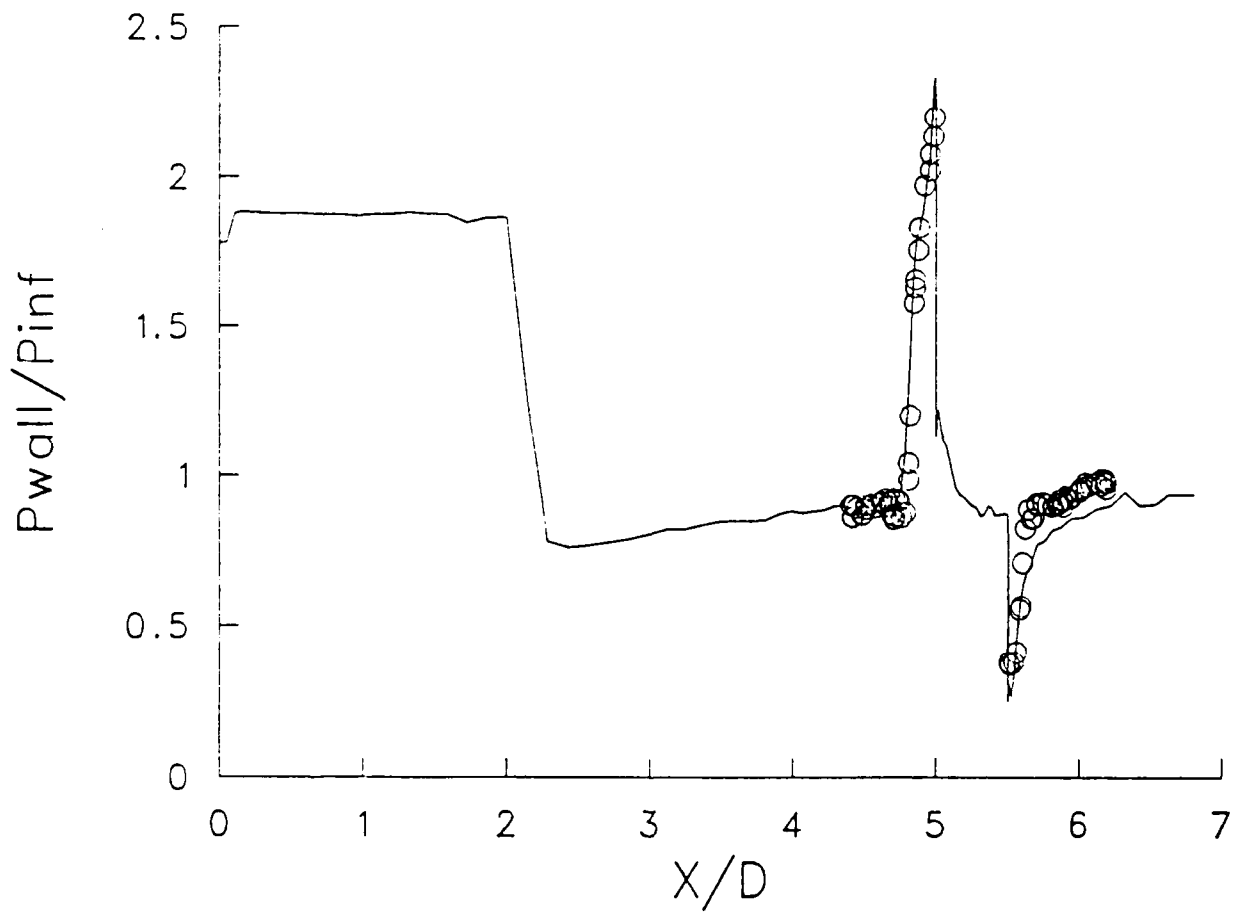


Figure 2. Comparison between computed and measured pressure distributions
(Mach number = 3.0, H/D = 0.04, Re = 1.33×10^6).

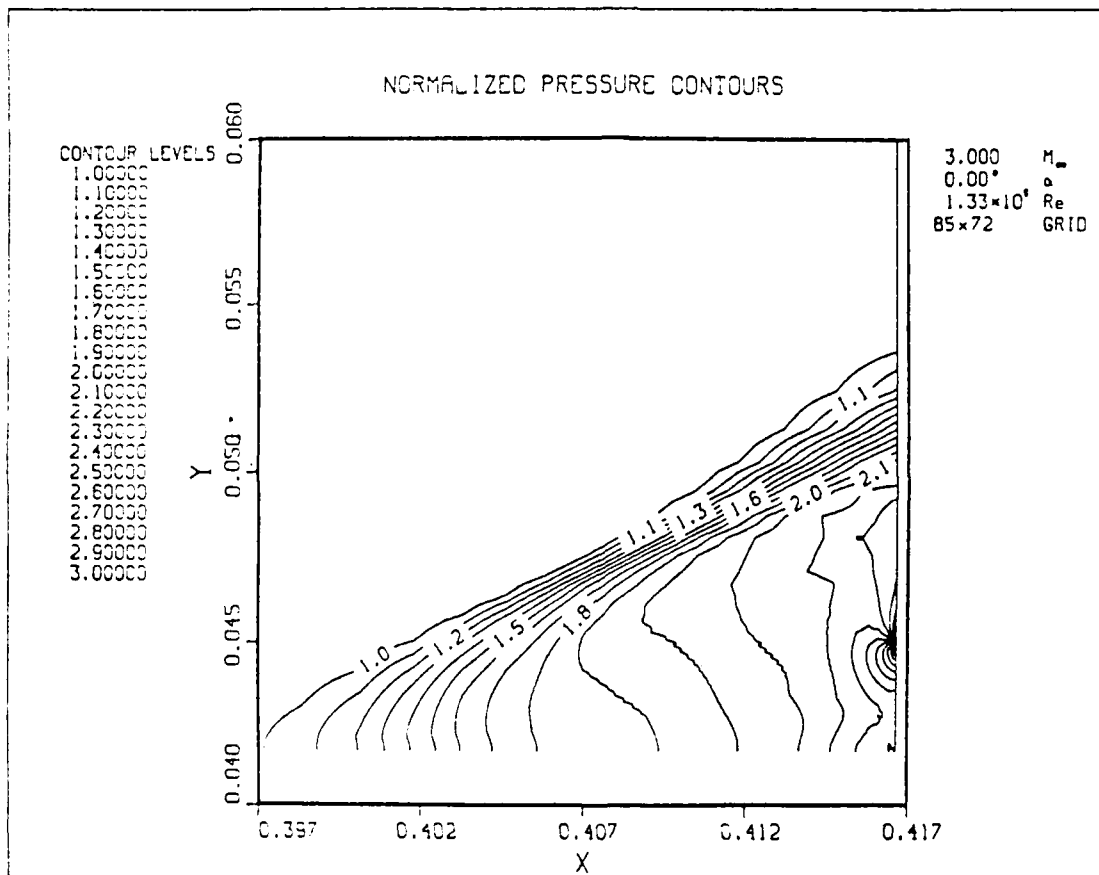


Figure 4. Pressure contours in separated flow region ahead of band
 (dimensions are in feet).

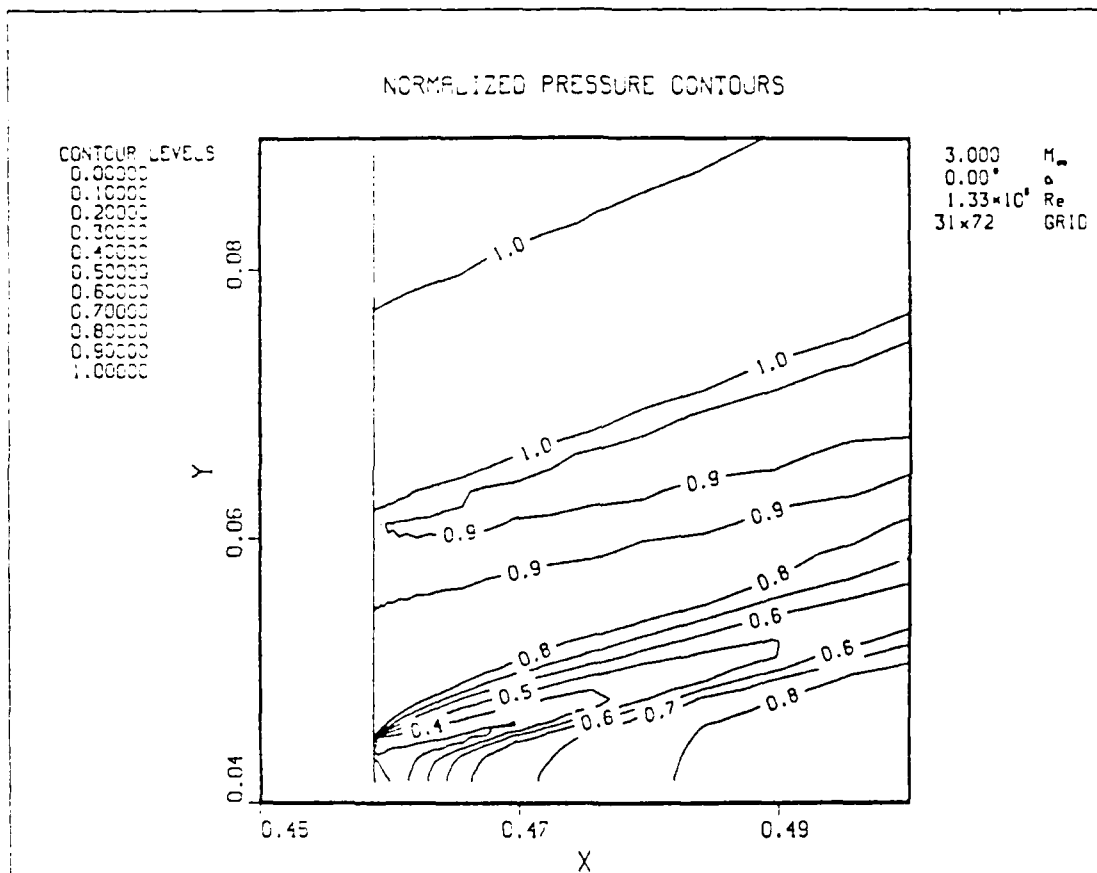


Figure 5. Pressure contours in separated flow region behind band
(dimensions are in feet).

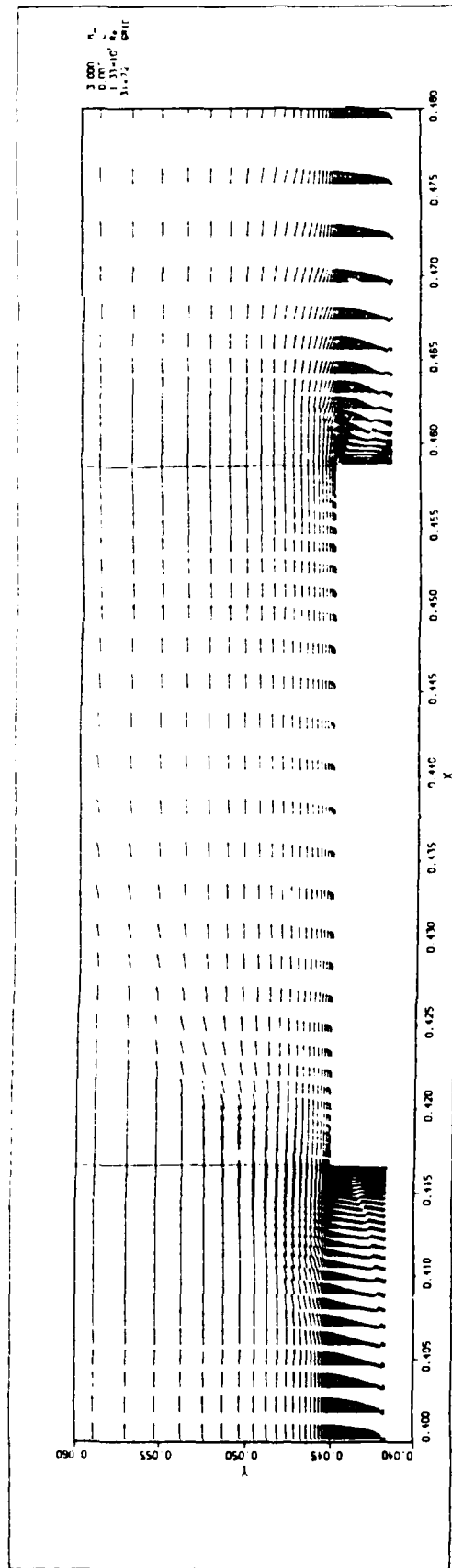


Figure 6. Velocity vector plot (dimensions are in ft).

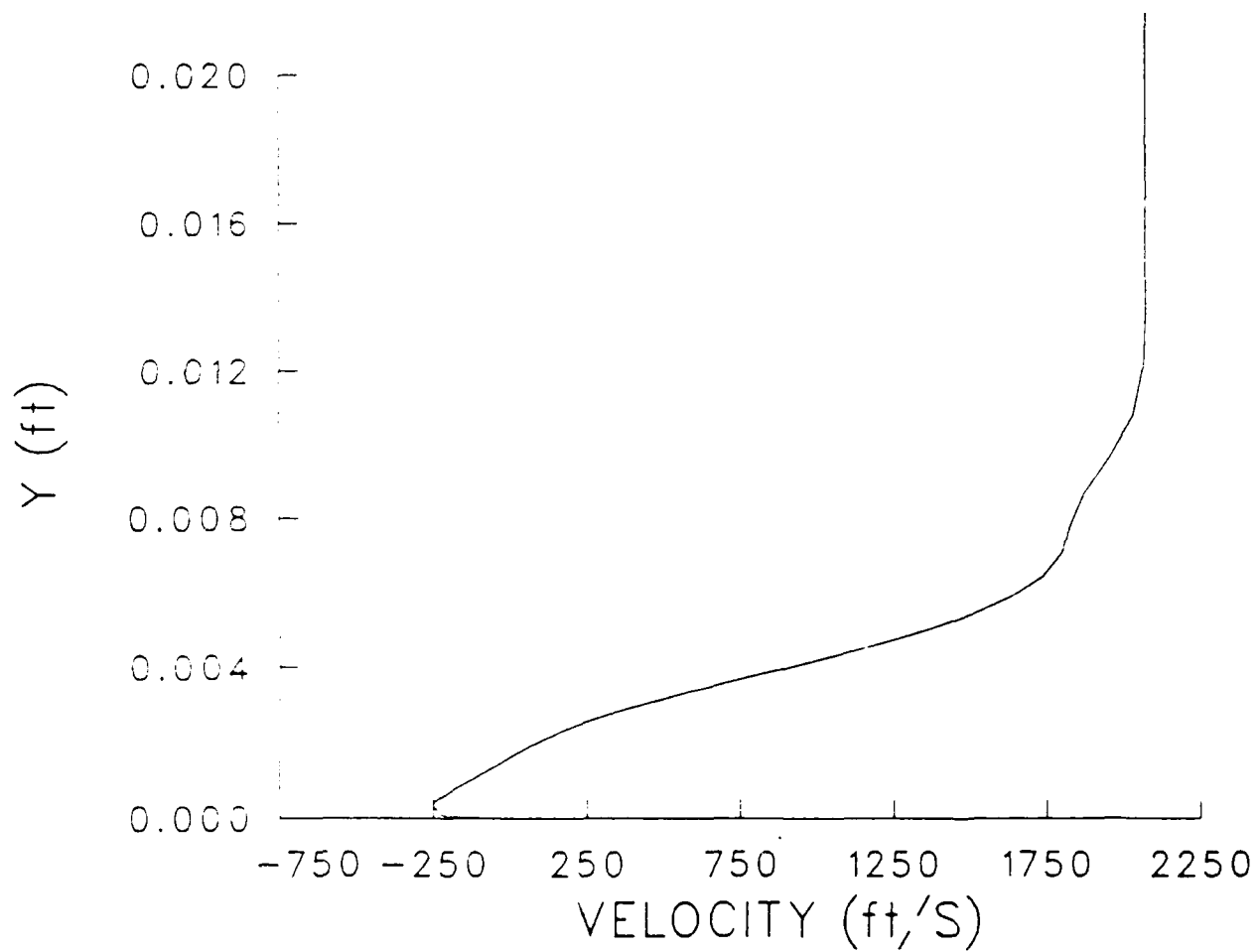


Figure 7. Velocity profile ahead of band ($\Delta X/H = 0.438$).

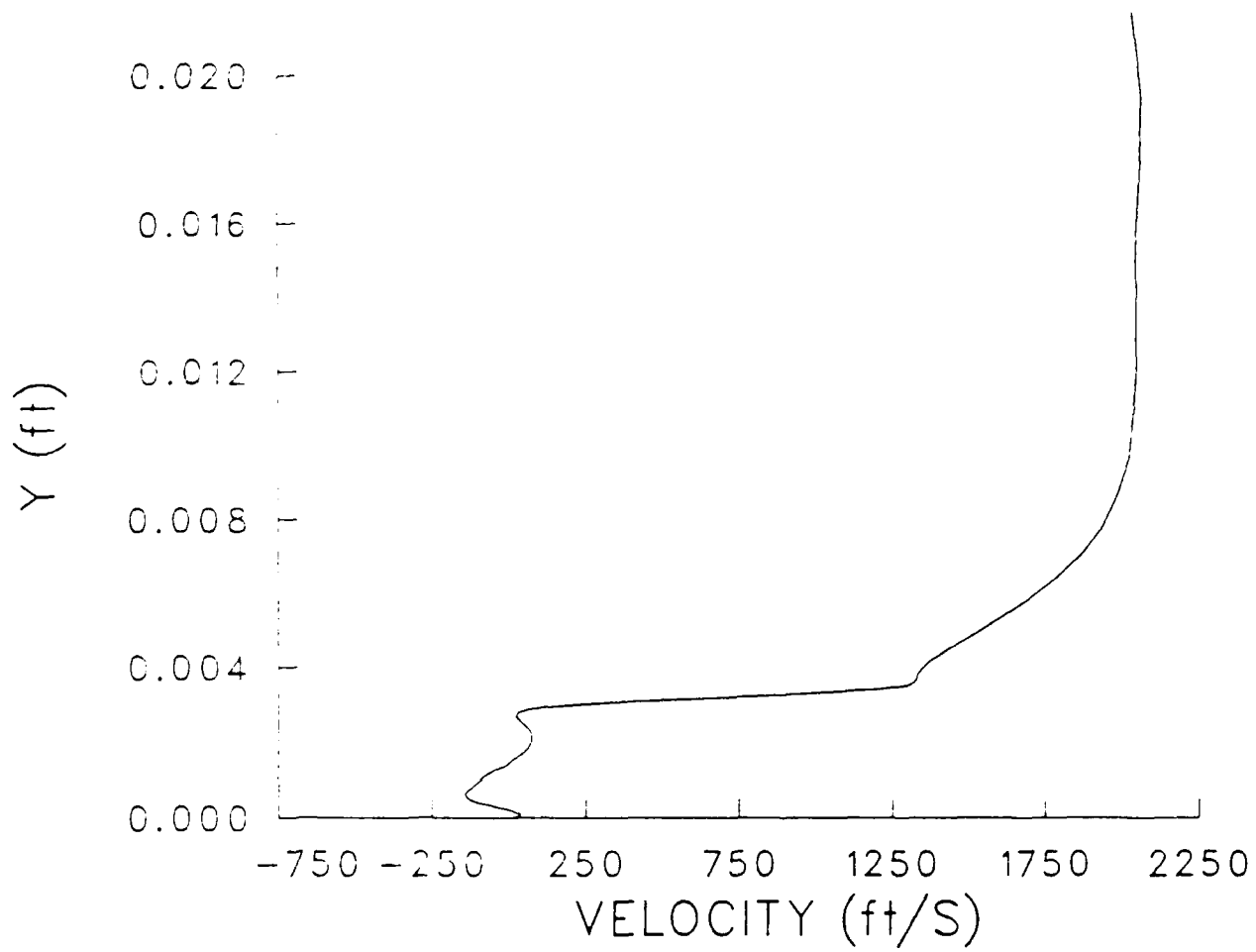


Figure 8. Velocity profile behind of band ($\Delta X/H = 0.10$).

References

1. Sahu, J and Danberg, J. E., "A Combined Computational and Experimental Study of Supersonic Flow Over a Protuberance," AIAA Paper No. 87-2291. Atmospheric Flight Mechanics Conference, Monterey, CA, August 1987.
2. Baldwin, B.S. and Lomax, H., "Thin Layer Approximation and Algebraic Model for Separated Turbulent Flows," AIAA Paper No. 78-257, AIAA 16th Aerospace Sciences Meeting, Huntsville, AL, January 1978.
3. Patel, N.R. and Sturek, W.B., "Multi-Tasked Numerical Simulations of Axisymmetric Ramjet Flows Using Zonal-Overlapped Grids," report to be published, U.S. Army Ballistic Research Laboratory, Aberdeen Proving Ground, Maryland.
4. Klebanoff, P. S., "Characteristics of Turbulence in a Boundary Layer with Zero Pressure Gradient," NACA Report 1247, 1955.
5. Clauser, F.H., "Turbulent Boundary Layers in Adverse Pressure Gradient," Journal of the Aeronautical Sciences, Vol. 21, No. 91, 1954.
6. Coles, D.E., "The Law of the Wake in the Turbulent Boundary Layer," Journal of Fluid Mechanics, Vol. 1, p. 191, 1956.
7. Coles, D.E., "The Turbulent Boundary Layer in a Compressible Fluid," Rand Corporation, Santa Monica, CA, Report R-403-PR, Appendix A, 1962.
8. White, F.M., Viscous Fluid Flow, McGraw-Hill, Inc. New York, New York, 1974.
9. Granville, P.S., "Baldwin-Lomax Factors for Turbulent Boundary Layers in Pressure Gradients," AIAA Journal, Vol. 25, No. 2, December 1987, pp. 1624-1627.
10. Moses, H.L., "The Behavior of Turbulent Boundary Layers in Adverse Pressure Gradients," Gas Turbine Laboratory, Massachusetts Institute of Technology, Cambridge, MA, Report No. 73, January 1964.
11. Nash, J.F., "Turbulent-Boundary-Layer Behavior and Auxiliary Equation," Recent Developments in Boundary Layer Research, AGARDograph 97, May 1965, pp. 253-279.
12. Visbal, M. and Knight, D., "The Baldwin-Lomax Turbulence Model for Two-Dimensional Shock-Wave/Boundary-Layer Interactions," AIAA Journal, Vol. 22, No. 7, July 1984.
13. Danberg, J.E. and Palko, K.L., "Measurement of Surface Pressures Caused by a Projectile Rotating Band at Supersonic Speeds," ARBRL-MR-3532, U.S. Army Ballistic Research Laboratory, Aberdeen Proving Ground, Maryland, July 1986, AD A171082.

INTENTIONALLY LEFT BLANK.

List of Symbols

A	= Van Driest damping constant
B	= constant in law of the wall
b	= half width of shear layer
C_{cp}	= constant (attached flow)
C_{kleb}	= constant in intermittency function
$C_{u,k}$	= constant (modifies C_{cp} for separated flows)
$F(y)$	= moment of vorticity
h	= displacement of shear layer from the wall
K	= Clauser constant
ℓ	= mixing length
Re	= Reynolds number based on body diameter
p	= pressure
U_d	= $\sqrt{(u^2 + v^2 + w^2)_{max}} - \sqrt{(u^2 + v^2 + w^2)_{min}}$
U_ϵ	= x-component of edge velocity
u	= local x-component of velocity
u_τ	= shear velocity = $\sqrt{\tau_w/\rho_w}$
v	= local y-component of velocity
w	= local z-component of velocity
x	= distance along the wall
y	= distance normal to the wall
y_m	= distance normal to the wall to the maximum in $F(y)$

Greek Symbols

β	= pressure gradient parameter
γ	= intermittency factor
δ	= boundary layer thickness
δ_k^*	= incompressible displacement thickness
η	= $\pi y/2\delta$
κ	= von Karman constant
μ	= dynamic viscosity
ν	= kinematic viscosity
Π	= Coles' turbulent boundary layer wake parameter
ρ	= density
τ	= shear stress
ω	= vorticity

Superscripts

i	= inner layer
o	= outer layer
+	= nondimensional using wall variables

Subscripts

e = boundary layer edge
min = distance from the wall to minimum in a variable
max = distance from the wall to maximum in a variable
n = normal
t = turbulent
w = wall

<u>No of Copies</u>	<u>Organization</u>	<u>No of Copies</u>	<u>Organization</u>
(Unclass., unlimited) 12	Administrator	1	Commander
(Unclass., limited) 2	Defense Technical Info Center		US Army Missile Command
(Classified) 2	ATTN: DTIC-DDA Cameron Station Alexandria, VA 22304-6145		ATTN: AMSMI-RD-CS-R (DOC) Redstone Arsenal, AL 35898-5010
1	HQDA (SARD-TR) WASH DC 20310-0001	1	Commander US Army Tank Automotive Command ATTN: AMSTA-TSL (Technical Library) Warren, MI 48397-5000
1	Commander US Army Materiel Command ATTN: AMCDRA-ST 5001 Eisenhower Avenue Alexandria, VA 22333-0001	1	Director US Army TRADOC Analysis Command ATTN: ATAA-SL White Sands Missile Range, NM 88002-5502
1	Commander US Army Laboratory Command ATTN: AMSLC-DL Adelphi, MD 20783-1145	(Class. only) 1	Commandant US Army Infantry School ATTN: ATSH-CD (Security Mgr.) Fort Benning, GA 31905-5660
2	Commander Armament RD&E Center US Army AMCCOM ATTN: SMCAR-MSI Picatinny Arsenal, NJ 07806-5000	(Unclass. only) 1	Commandant US Army Infantry School ATTN: ATSH-CD-CSO-OR Fort Benning, GA 31905-5660
2	Commander Armament RD&E Center US Army AMCCOM ATTN: SMCAR-TDC Picatinny Arsenal, NJ 07806-5000	(Class. only) 1	The Rand Corporation P.O. Box 2138 Santa Monica, CA 90401-2138
1	Director Benet Weapons Laboratory Armament RD&E Center US Army AMCCOM ATTN: SMCAR-LCB-TL Watervliet, NY 12189-4050	1	Air Force Armament Laboratory ATTN: AFATL/DLODL Eglin AFB, FL 32542-5000
1	Commander US Army Armament, Munitions and Chemical Command ATTN: SMCAR-ESP-L Rock Island, IL 61299-5000		<u>Aberdeen Proving Ground</u> Dir, USAMSAA ATTN: AMXSY-D AMXSY-MP, H. Cohen Cdr, USATECOM ATTN: AMSTE-TO-F Cdr, CRDEC, AMCCOM ATTN: SMCCR-RSP-A SMCCR-MU SMCCR-MSI Dir, VLAMO ATTN: AMSLC-VL-D
1	Commander US Army Aviation Systems Command ATTN: AMSAV-DACL 4300 Goodfellow Blvd. St. Louis, MO 63120-1798		
1	Director US Army Aviation Research and Technology Activity Ames Research Center Moffett Field, CA 94035-1099		

DISTRIBUTION LIST

<u>No.</u> <u>Copies</u>	<u>Organization</u>	<u>No.</u> <u>Copies</u>	<u>Organization</u>
1	Commander US Army Missile Command ATTN: B. Walker Redstone Arsenal, AL 35898-5010	6	Commander U.S. Army Armament Research, Development & Engineering Center ATTN: SMCAR-TSS SMCAR-LCA-F J. Grau R. Kline S. Kahn H. Hudgins Picatinny Arsenal, NJ 07806-5000
3	Commander Naval Surface Weapons Center ATTN: Code R44 (Dr. F. Priolo) Code R44 (Dr. A. Wardlaw) K-24, Building 402-12 White Oak Laboratory Silver Spring, MD 20903-5000	6	Director National Aeronautics and Space Administration Ames Research Center ATTN: MS-227-8, L. Schiff MS-258-1, T. Holst MS-258-1, J. Steger MS-258-1, D. Chaussee MS-258-1, M. Rai MS-229-1 M. Rubesin Moffett Field, CA 94035
5	Director National Aeronautics and Space Administration Langley Research Center ATTN: Tech Library Mr. P. J. Bobbitt Mr. D. M. Bushnell Dr. M. J. Hensch Dr. I. E. Beckwith Langley Station Hampton, VA 23665	1	Air Force Armament Laboratory ATTN: AFATL/FXA (Stephen C. Korn) Eglin AFB, FL 32542-5434
1	United States Military Academy Department of Mechanics ATTN: LTC Andrew L. Dull West Point, NY 10996	2	USAF Wright Aeronautical Laboratories ATTN: AFWAL/FIMG Mr. Norman E. Scaggs Dr. J. Shang WPAFB, OH 45433-6553
1	Commander US Naval Surface Weapons Center ATTN: Dr. F. Moore Dahlgren, VA 22448		

DISTRIBUTION LIST

<u>No.</u> <u>Copies</u>	<u>Organization</u>	<u>No.</u> <u>Copies</u>	<u>Organization</u>
1	Massachusetts Institute of Technology ATTN: Tech Library 77 Massachusetts Avenue Cambridge, MA 02139	1	University of Maryland Department of Aerospace Engr. ATTN: Dr. J. D. Anderson, Jr. College Park, MD 20742
1	AEDC Calspan Field Service ATTN: MS 600 (Dr. John Benek) AAFS, TN 37389	1	University of Notre Dame Department of Aeronautical and Mechanical Engineering ATTN: Prof. T. J. Mueller Notre Dame, IN 46556
1	Virginia Polytechnic Institutue & State University ATTN: Dr. Clark H. Lewis Department of Aerospace & Ocean Engineering Blacksburg, VA 24061	1	University of Texas Department of Aerospace Engineering and Engineering Mechanics ATTN: Dr. D. S. Dolling Austin, Texas 78712-1055
1	University of California, Davis Department of Mechanical Engineering ATTN: Prof. H.A. Dwyer Davis, CA 95616	2	University of Delaware Department of Mechanical Engineering ATTN: Dr. John Meakin, Chairman Dr. Barry Sidel Newark, DE 19716
1	Pennsylvania State University Department of Aerospace Engineering ATTN: Dr. G. S. Dulikravich University Park, PA 16802	1	University of Florida Department of Engineering Sciences College of Engineering ATTN: Prof. C. C. Hsu Gainesville, FL 32611
1	University of illinois at Urbana Champaign Department of Mechanical and Industrial Engineering Urbana, IL 61801	1	Advanced Technology Center Arvin/Calspan Aerodynamics Research Department ATTN: Dr. M. S. Holden P. O. Box 400 Buffalo, NY 14225

DISTRIBUTION LIST

<u>No.</u> <u>Copies</u>	<u>Organization</u>	<u>No.</u> <u>Copies</u>	<u>Organization</u>
1	Mississippi State University Mechanical Engineering Department ATTN: Dr. B. K. Hodge Mississippi State, MS 39762	2	Ford Aerospace and Communications Corporation Aeronutronics Division ATTN: Charles White Bud Blair Ford Road Newpoint Beach, CA 92658
2	David Taylor Research Center ATTN: Dr. P. S. Granville Dr. de los Santos Bethesda, MD 20084	1	University of Cincinnati Department of Aerospace Engineering ATTN: Prof. Stanley Rubin Mail Location 70 Cincinnati, OH 45221
2	Director Sandia National Laboratories ATTN: Dr. W. Oberkampf Dr. F. Blottner Division 1636 Albuquerque, NM 87185	1	Illinois Institute of Technology College of Engineering Fluid Dynamics Research Center ATTN: Dr. Mukund Acharya IIT Center Chicago, IL 60616
1	The University of Arizona Aerospace Engineering Department ATTN: Prof. I. Wygnanski Tucson, AZ 85721	1	University of New Mexico Department of Mechanical Engineering ATTN: Dr. C. Randall Truman Albuquerque, New Mexico 87131
1	Applied Technology Associates ATTN: Mr. R. J. Cavalleri P.O. Box 19434 Orlando, FL 32814	1	Lawrence Livermore National Laboratory Center for Compressible Turbulence ATTN: Dr. A. C. Buckingham MS/L-16 P. O. Box 808 Livermore, CA 94550
1	United Technologies Corporation Chemical Systems Division ATTN: Mr. A. L. Holzman P.O. Box 50015 600 Metcalf Road San Jose, CA 95150-0015	1	Widener University Department of Mechanical Engineering ATTN: Dr. Robert M. Hartman Chester, PA 19013
2	Honeywell Inc. ATTN: Wilford E. Martwick Ken Sundeen 600 Second Street, North East Hopkins, MN 55343		

USER EVALUATION SHEET/CHANGE OF ADDRESS

This laboratory undertakes a continuing effort to improve the quality of the reports it publishes. Your comments/answers below will aid us in our efforts.

1. Does this report satisfy a need? (Comment on purpose, related project, or other area of interest for which the report will be used.) _____

2. How, specifically, is the report being used? (Information source, design data, procedure, source of ideas, etc.) _____

3. Has the information in this report led to any quantitative savings as far as man-hours or dollars saved, operating costs avoided, or efficiencies achieved, etc? If so, please elaborate. _____

4. General Comments. What do you think should be changed to improve future reports? (Indicate changes to organization, technical content, format, etc.) _____

BRL Report Number _____ Division Symbol _____

Check here if desire to be removed from distribution list. _____

Check here for address change. _____

Current address: Organization _____
Address _____

-----FOLD AND TAPE CLOSED-----

Director
U.S. Army Ballistic Research Laboratory
ATTN: SLCBR-DD-T
Aberdeen Proving Ground, MD 21005-5066

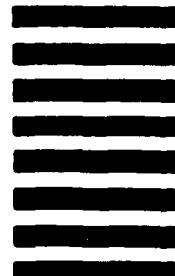
OFFICIAL BUSINESS



NO POSTAGE
NECESSARY
IF MAILED
IN THE
UNITED STATES

BUSINESS REPLY LABEL
FIRST CLASS PERMIT NO 12067 WASHINGTON D C

POSTAGE WILL BE PAID BY DEPARTMENT OF THE ARMY



Director
U.S. Army Ballistic Research Laboratory
ATTN: SLCBR-DD-T
Aberdeen Proving Ground, MD 21005-9989